Research Article Vol. 7, No. 8 / August 2020 / Optica 965

optica

Buildup and dissociation dynamics of dissipative optical soliton molecules

YI ZHOU, YU-XUAN REN, JIAWEI SHI, HUADE MAO, AND KENNETH K. Y. WONG*

Department of Electrical and Electronic Engineering, The University of Hong Kong, Pokfulam Road, Hong Kong, China
**Corresponding author: kywong@eee.hku.hk*

Received 8 April 2020; revised 6 July 2020; accepted 16 July 2020 (Doc. ID 394706); published 7 August 2020

Solitons can self-assemble into stable bound states, also denoted as soliton molecules that exhibit molecule-like dynamics. Soliton molecules have been predominantly investigated in the anomalous dispersion mode-locked fiber lasers. However, the soliton molecule dynamic evolution is still largely unexplored in the normal dispersion regime. We reveal here that, in the normal dispersion regime, the buildup and dissociation dynamics of soliton molecules. Our theoretical prediction indicates that, under different transmission functions of a saturable absorber (SA), a pair of solitons can be formed directly from background noise and then evolve into a soliton molecule through intense repulsive interaction, or a soliton molecule can be triggered to dissociate into a single soliton with transient annihilation and energy transfer. The experimental observation of short-time soliton molecule buildup and a new soliton molecule dissociation process corroborate the theoretical prediction. Furthermore, a long-time soliton molecule buildup (∼900 ms) is discovered with single soliton splitting and soliton pair attraction. The buildup time is over four orders of magnitude longer than that of the short-time soliton molecule (∼21 μs). Our work unveils new perspectives into the ultrafast transient process and the interaction dynamics of soliton molecules in complex nonlinear systems.

https://doi.org/10.1364/OPTICA.394706

1. INTRODUCTION

The soliton, as a remarkably localized structure in nonlinear systems, has attracted considerable attention in numerous contexts, including fluids, plasmas, fibers, optical systems, polymers, and Bose–Einstein condensates [1–5]. The soliton in the dissipative system suffers from the balance between nonlinearity and dispersion; the existence and stability of dissipative solitons highly depend on the interplay between gain and loss [6]. The mode-locked fiber lasers, as an absolutely dissipative system, provide an excellent test bed rich in dissipative soliton dynamics, such as soliton molecule [7], optical rogue wave [8], soliton explosion [9], and triple-state dissipative soliton switching [10]. In the past, achieving a temporally and spectrally resolved study of the transient soliton dynamics is always a challenge because every transient event possesses a singular occurrence with a unique spectral-temporal feature. While recently developed, the time-stretch dispersive Fourier transform (TS-DFT) technique provides a powerful way for real-time, single-shot measurement of ultrafast dynamical phenomena [11].

The TS-DFT technique helps scientists to experimentally resolve the variety of soliton transient evolution. In particular, the soliton molecules that exhibit fascinating particle-like interactions, e.g., vibration, synthesis, and dissociation, constitute the fundamental problems in soliton physics [12–17]. In terms of application, soliton molecules may increase the capacity of telecommunication, which is also attractive in all-optical information storage [18,19]. The formation of a single soliton refers to the universal behavior of many nonlinear systems corresponding to the law of 'survival of the strongest' [20]. In this respect, the formation of soliton molecules may result from soliton splitting [21], soliton shaping of the background noise [22], relaxed oscillation, or Q-switch lasing [23,24]. In general, soliton molecules displayed rich dynamics in the anomalous dispersion mode-locked fiber laser, including different initial formation conditions [16,25]. In addition to stationary soliton molecules, there are also dynamic soliton molecules, among which the time interval or phase difference between individual solitons changes over time [13,26].

Despite the soliton molecules buildup that has been reported in the anomalous dispersion regimes previously, it is still a crucial question on how initial noise evolves into a soliton molecule, particularly in the normal dispersion regime of mode-locked fiber laser being largely unexplored, which is an excellent platform for dissipative solitons involving rare dynamics. Numerical studies use well-separated solitons instead of noise as the initial conditions for studying the generation of soliton molecules, which may ignore the non-trivial nonlinear processes involved [27]. In the anomalous dispersion regime, the soliton molecules are the consequences of oscillation between the soliton tail. Such oscillations are produced by the Kelly sideband and have been confirmed by experiments [28,29]. Conversely, there is no Kelly sideband in the normal dispersion regime, which could suggest the existence of different

dynamics of soliton molecules. Other than the buildup process, it is a great interest to explore the different dynamical processes like the dissociation of soliton molecules in a normal dispersion ultrafast laser. The probe and trigger of the dynamical soliton molecule buildup and dissociation in the normal dispersion dissipative systems may contribute to control and generate ultrashort solitons in an optical oscillator, further extending the 'molecular' analogy and potential applications.

Here, we reveal the buildup and dissociation dynamics of dissipative soliton molecules in the normal dispersion mode-locked fiber laser. Numerical simulation suggests that soliton molecule buildup depends sensitively on initial conditions; the parameter change of the saturable absorber (SA) will trigger the soliton molecule dissociation. The precise control of the polarization setting and gain of the laser in combination with accurate TS-DFT detection allows us to experimentally corroborate the theoretical prediction. Specifically, the soliton molecule buildup processes from background noise in both short and long-time scales and a new soliton dissociation process have been observed in the normal dispersion fiber laser. These results unveil the diversity of soliton molecule interaction in a mode-locked fiber laser, empowering the understanding of complex dynamics in nonlinear optical systems.

2. NUMERICAL SIMULATION

Soliton molecules buildup and dissociation manifest a rich set of soliton interactions, including attraction, repulsion, collision, vibration, and annihilation in anomalous dispersion ultrafast fiber lasers. The interaction between solitons is mainly through dispersive waves [22]. However, dispersive waves generally do not present in normal dispersion mode-locked fiber lasers, which could suggest a different interaction mechanism of soliton molecules, and the interactions could arise from gain depletion and recovery [30,31]. Further, soliton molecules' buildup and dissociation could originate from different dynamics in the normal dispersion regime. With the above mechanism in mind, it is intuitive to execute a numerical simulation to explore the buildup and dissociation process in a normal dispersion ultrafast fiber laser. In the simulation, nonlinear polarization rotation (NPR) is used to achieve mode-locking pulse generation. The laser architecture comprises an erbium-doped fiber (EDF) with normal dispersion at 1.56 μm (amplification medium), two sections of single-mode fiber (SMF) with anomalous dispersion, a SA, and an output coupler (OC). Pulse propagation within the fiber is modeled with a modified nonlinear Schrödinger equation for the slowly varying pulse envelope:

$$\frac{\partial \varphi}{z} = -\frac{i}{2}\beta_2 \frac{\partial^2 \varphi}{\partial t^2} + \frac{g}{2\Omega^2}\frac{\partial^2 \varphi}{\partial t^2} + i\gamma|\varphi|^2\varphi + \frac{g}{2}\varphi. \quad (1)$$

Here, β_2 is group-velocity dispersion (GVD), and γ is the coefficient of cubic nonlinearity for the fiber segment. The dissipative terms represent linear gain as well as a Gaussian approximation to the gain profile with the bandwidth Ω. The gain is described by $g = g_0 \exp(-E_p/E_s)$, where g_0 is the small signal gain, which is non-zero only for the gain fiber, E_p is the pulse energy, and E_s is the gain saturation energy determined by pump power. The parameters used in the numerical simulations are following typical experimental values.

Buildup and dissociation of soliton molecules belong to different dynamics. We hypothesize that the variation of polarization settings could trigger these dynamics at fixed gain. The varied polarization indicates that the transmission functions of the NPR are different [25,32]. Based on this assumption, we choose different SA transmission functions that correspond to the soliton molecule buildup and dissociation. For the soliton molecule buildup, the SA transmission function is $T = R_0 + \Delta R(1 - 1/(1 + P/P_0))$; for the dissociation process, the corresponding transmission function is $T = R_0 + \Delta R \sin^2(0.5\pi \times P/P_0)$, where R_0 is the unsaturated reflectance, ΔR is the saturable reflectance, P is the pulse instantaneous power, and P_0 is the saturation power. Other parameters are chosen according to the experimental components: $\Omega = 40$ nm, $\lambda_0 = 1560$ nm, $E_s = 10.8$ pJ, $g_0 = 4.5\ \mathrm{m}^{-1}$, $\beta_2 = 6.5\ \mathrm{ps}^2/\mathrm{km}$, and $\gamma = 6.6\ \mathrm{W}^{-1}\ \mathrm{km}^{-1}$ for EDF; $\beta_2 = -21\ \mathrm{ps}^2/\mathrm{km}$ and $\gamma = 1.65\ \mathrm{W}^{-1}\ \mathrm{km}^{-1}$ for SMF1; $\beta_2 = -10.4\ \mathrm{ps}^2/\mathrm{km}$ and $\gamma = 1.65\ \mathrm{W}^{-1}\ \mathrm{km}^{-1}$ for SMF2; $R_0 = 0.10$.

As the soliton dynamics are closely related to the transmission function, gain, and the initial condition, a scalar iterative map was calculated to identify the regimes for soliton molecule buildup and dissociation [17]. We systematically varied the SA parameter and fixed gain setting to identify stability regimes with qualitatively different behavior. The iterative map for soliton molecule buildup evolution is shown in Fig. 1(a); the initial condition is single, and two weak sech-shape pulses combine with random noise. The soliton dissociation map is modeled with random noise overlaid on two sech-shape pulses (dual solitons) as minute perturbation [Fig. 1(b)]. The parameter spaces were finely gridded, and the behavior of the simulation moves towards either convergence or instability. In most cases, the system reaches steady-state after hundreds of roundtrips (RTs). The blue region in the figure corresponds to convergence towards a stable single pulse, which is not sensitive to the initial condition: by slightly changing the initial seed intensity or pulse separation, even if seeded from noise, the simulation will still converge to the final state under certain parameters. The orange region corresponds to either a stable single pulse or molecules depending on initial conditions. The simulations converging to either single or double pulses are sensitive to the initial pulse number and particular noise on the seed. The

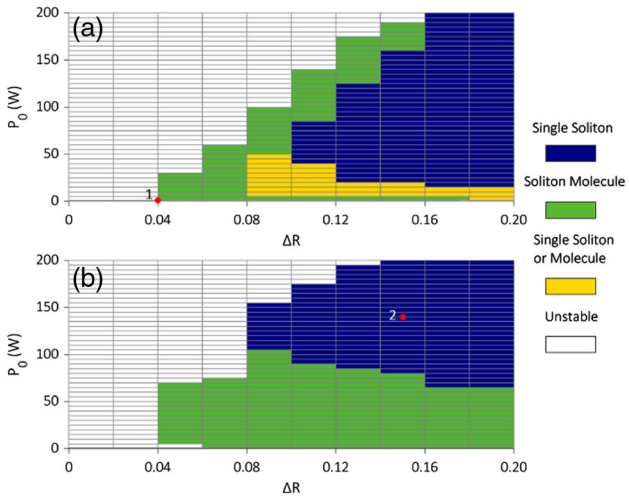

Fig. 1. Stability regimes as a function of saturable absorber parameters (ΔR, P_0) at fixed $E_s = 10.8$ pJ and $g_0 = 4.5\ \mathrm{m}^{-1}$ for (a) soliton molecule buildup and (b) soliton molecule dissociation. The colored legend describes the different regimes. The red points (1) and (2) correspond to the simulations in Figs. 2 and 3, respectively.

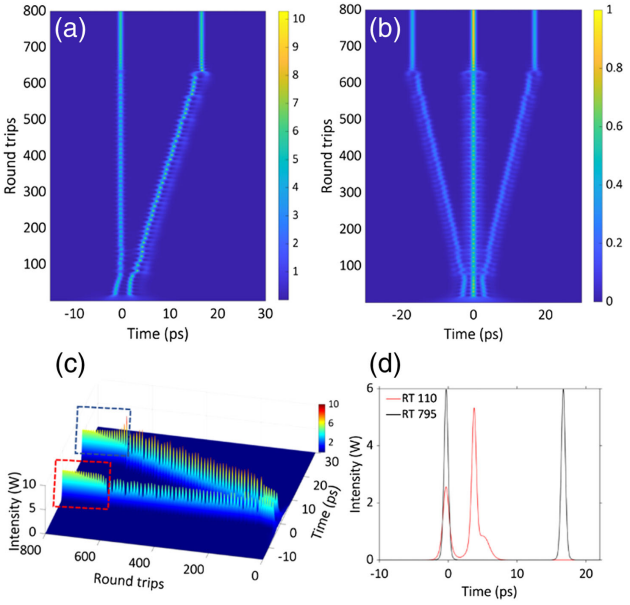

Fig. 2. Soliton molecule buildup through repulsion [corresponding to point 1 in Fig. 1(a)]. (a) Temporal evolutions in the soliton molecule buildup process. (b) The corresponding field autocorrelation evolution. (c) Side view of (a). (d) Temporal intensity of soliton molecule at RT numbers of 110 and 795.

green region corresponds to only stable soliton molecules that is irrespective of the initial condition (single or dual pulse seed for the soliton buildup).

By varying SA parameters, the model suggests many phenomena. Both attraction and repulsion of soliton molecules are observed in the settings. Specifically, we choose two peculiar dynamical processes that correspond to soliton molecule buildup and dissociation, respectively. Mode locking and soliton repulsion are observed in the soliton molecule buildup that is evidenced in the temporal evolution [Fig. 2(a)] and field autocorrelation trace [Fig. 2(b)] with $\Delta R = 0.04$ and $P_0 = 1$ W [Point 1 in Fig. 1(a)]. The initial separation of pulses is 4 ps, and the repulsive process persists for ~600 RTs before reaching a stable soliton molecule. We find that the two initial pulses formed from background noise have a large difference in intensity, and the initial pulse separation is much smaller than the final stable value, resulting in a strong repulsive effect. This repulsive evolution depends sensitively on initial conditions and can only be reproduced when the gain saturation energy E_s, ΔR, and P_0 are maintained in a very narrow region.

The interaction of solitons refers to long-range interactions that arise from gain depletion and recovery. As a result, the pulses experience a time-dependent gain and have a drift velocity that is proportional to the pulse energy [33]. In the initial stage of the repulsion, the trailing pulse exerts higher energy than the leading pulse [RT 110 in Fig. 2(d)]. However, the leading soliton depletes the gain of a laser, resulting in less gain for a tailing soliton until it is recovered to the value before the leading soliton. The gain differential that determines the magnitude of the soliton drift velocity is proportional to the pulse energy. Therefore, the trailing pulse possesses larger drifting velocity in comparison to the leading pulse that only drifts 0.25 ps in repulsive evolution. A significant twist at the RT number of 635 is due to the rapidly reducing energy difference in the leading pulse and the trailing pulse, which leads to the gain difference, and the relative speed of the two pulses begin to

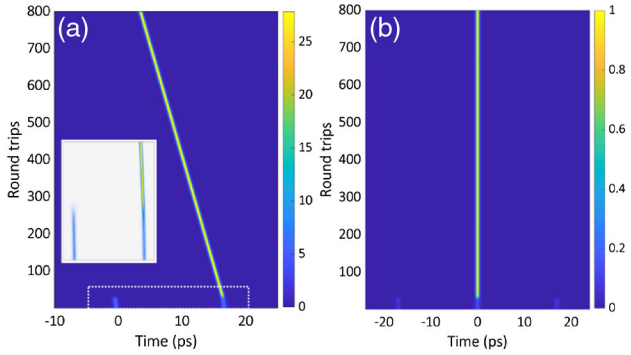

Fig. 3. Simulation of soliton molecule dissociation [corresponding to point 2 in Fig. 1(b)]. (a) Temporal evolutions in the soliton molecule dissociation process. (b) The corresponding field autocorrelation evolution.

rapidly decrease to a negligible level [dashed rectangle in Fig. 2(c) and RT 795 in Fig. 2(d)]. The repulsive force gradually weakens in the kink process and can be neglected when the pulses enter the stagnation point. Eventually, the two pulses maintained almost fixed temporal separation.

The soliton molecule dissociation corresponds to point 2 in Fig. 1(b) with $\Delta R = 0.15$ and $P_0 = 140$ W, while the simulation temporal evolutions and field autocorrelation traces are shown in Figs. 3(a) and 3(b). Owing to polarization perturbation, the corresponding transmission function of NPR with greater modulation depth and saturation power triggers the soliton molecule to dissociate into a single soliton. The inset for the zoom-in of the dashed rectangle in Fig. 3(a) shows some exotic dynamic phenomena, e.g., leading soliton transient annihilation, energy transfer, and trailing soliton temporal drift.

3. EXPERIMENTAL RESULTS AND DISCUSSION

Next, we performed experiments based on the parameters used in the simulation to validate the buildup and dissociation dynamics of soliton molecules in a normal dispersion ultrafast fiber laser. The laser consists of a segment of EDF (Lucent-SFD), two polarization controllers (PC), some SMF pigtails, and an optical integrated module (OIM) that includes a polarization-dependent isolator, a wavelength division multiplexer (WDM), and a 10:90 OC (Fig. 4). The 6 m EDF acts as the gain medium, while another piece of ~2 m SMF, including 1 m Hi-1060 fiber and 1 m SMF-28e fiber, extends the cavity length and provides a net cavity dispersion of ~0.02 ps^2 and repetition rate of 25 MHz. The temporal information was detected by a 20 GHz photodiode (PD1, Agilent 83440C) and digitized by a 20 GHz real-time oscilloscope (Lecroy SDA 820Zi-B), while the optical spectrum was recorded by an optical spectrum analyzer (OSA, YOKOGAWA AQ6370D) and the real-time oscilloscope using TS-DFT simultaneously. The dispersive Fourier transform (DFT) branch was composed of a spool of dispersion-compensating fiber (DCF) with −577 ps/nm dispersion and detected by a 12 GHz photodiode (PD2, New Focus 1544-B), with a single-shot spectrum resolution of 0.17 nm [34]. During the experiment, the pump power could be turned on when the PCs were preset in the settings, generating soliton molecules, and the oscilloscope was triggered to record the transient signal. We measured the buildup and dissociation process of soliton molecules during the experiments, as described below.

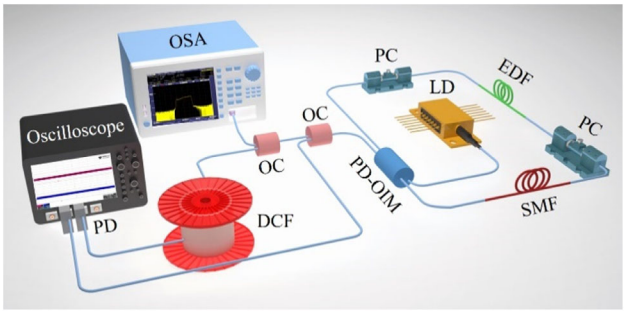

Fig. 4. Schematic diagram of the experiment setup. EDF, erbium-doped fiber; SMF, single-mode fiber; PC, polarization controller; LD, laser diode; PD-OIM, polarization-dependent optical integrated module; OSA, optical spectrum analyzer; DCF, dispersion-compensation fiber.

A. Short-Time Soliton Molecule Formation Dynamics

Experimentally, short-time and long-time soliton molecule buildup processes were observed at different polarization settings. First, we recorded a soliton molecule corresponding to a short-time buildup process and explored its formation dynamics. Figure 5 shows the experimental result for short-time soliton molecule formation. The measured DFT spectra [Fig. 5(a)] exhibit drastic changes before a stable soliton molecule is formed. In previous reports [16,25], a single soliton experiences a soliton split and complex multi-pulse evolution before the stable soliton molecules are established. However, in this experiment, two pulses directly formed at the initial stage [Fig. 5(b)] with no information on the dynamic single soliton split process, and the pulses underwent a strong repulsion, before the stable formation of a soliton molecule. The close-up view of the region [Fig. 5(d)] between 1560–1565 nm [zoom-in plot of dashed rectangle in Fig. 5(a)] suggests a slight sliding phase in the pulse evolution while keeping fixed temporal separation, which is attributed to spectral fringe sliding toward higher frequencies as RTs are increased [13,35].

The solitons interactions can be revealed by first-order field autocorrelation, which has been used to probe the evolving separation between bound solitons and capture the transient ordering of incoherent dissipative solitons. The Fourier transforms of the single-shot spectra in Fig. 5(a) provided the field autocorrelation traces [Fig. 5(b)]. Mode-locking begins near a RT number of 1600, producing two solitons from background noise directly, the initial separation of the two solitons was 4.3 ps. Then, the significant repulsive stage lasts ≈540 RTs for two solitons, eventually resulting in a stable separation of 42 ps at the RT number of 2140. The energy evolution [black line overlaid in Fig. 5(b)] was calculated by integrating the measured spectra over the entire spectra band. There is an energy overshoot in the figure, which characterizes the mode-locking transition; then, the energy decreases while the solitons repel each other, and, finally, the energy is stabilized. The cross section of the field autocorrelation trace at the RT number of 2500 [Fig. 5(c)] corresponds to a period of the spectral modulation of 0.182 nm, and the two pulses separated with 42 ps temporal separation. In contrast, the pulse duration was measured by an

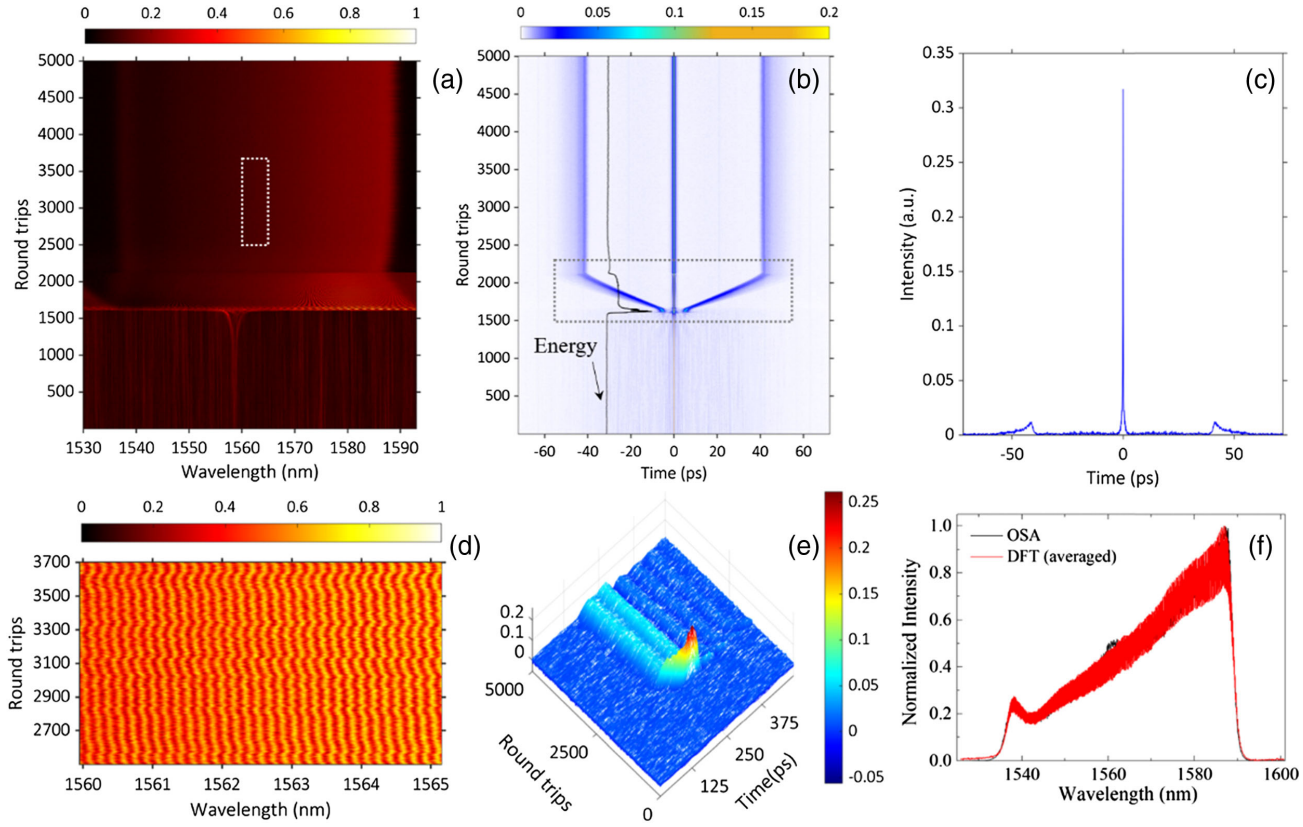

Fig. 5. Short-time soliton molecule formation from background noise. (a) The real-time spectral evolution measured via DFT. (b) The field autocorrelation traces calculated via the Fourier transform of each single-shot spectra in (a), the black line shows the energy evolution. (c) Field autocorrelation traces at RT number of 2500. (d) Zoom-in plot of dashed rectangle in (a). (e) The corresponding temporal intensity evolutions measured by a photodetector. (f) The good agreement between the spectra measured by OSA (black) and the average spectrum calculated from 1000 single-shot spectra (red) under stable mode-locking confirms the accuracy of TS-DFT.

autocorrelator (Femtochrome, FR-102 MN) to be 0.3 ps, which suggests that the interactions of the soliton molecule refer to weak long-range interactions (the separation between the solitons is 140 times that of the pulse width) [36]. The weak side lobes on both sides of the autocorrelation trace [Fig. 5(c)] also confirm the weak interaction.

Figs. 2(b) and 5(b) both show the mode-locking and soliton repulsive process. The initial separation of pulses of 4 ps and the repulsive last ~600 RTs in simulation [Fig. 2(b)] agree well with the experimental values. The instant kink also occurs at RT 2140 in the experiment [Fig. 5(b)]. During the twisting process, the intensity of the main autocorrelation peak will be further reduced due to the energy redistribution of the two pulses in the time domain. The only difference is that the two solitons in Fig. 2(b) showed more obvious breathing behavior in the repulsion evolution in contrast to the experiment. Due to the weak long-range interactions of soliton molecules corresponding to a larger pulses temporal interval leading to the very weak intensity of sidelobes in the autocorrelation trace [Fig. 5(b)], breathing behavior is not easily observable. However, the energy oscillation exists in the repulsion process of the soliton molecule [RTs 1700–2100 on the black line in Fig. 5(b)], indicating that the soliton molecule may also manifest similar breathing behavior in the experiment. Figure 5(e) shows the corresponding temporal intensity evolutions measured by the photodetector. The average spectrum calculated from 1000 single-shot spectra (red curve) matches well with the spectrum recorded on the OSA (black curve) [Fig. 5(f)], suggesting a fine mapping of the ultrafast optical spectrum associated with the dispersion [37]. Therefore, it also confirms that the TS-DFT technique can accurately map the spectral information of soliton molecules into the temporal domain.

Rich soliton interactions include the alternating soliton attraction, repulsion, and vibration during soliton molecule formation that exists in an anomalous dispersion ultrafast fiber laser [25], or only attractive interaction was discovered during soliton molecule formation in a Ti:sapphire laser [26]. In contrast, our work shows a completely different character in a normal dispersion mode-locked fiber laser. Repulsion dominates the interaction of soliton molecules and lacks the splitting process of a single soliton, highlighting the difference among the systems with variable net cavity dispersion. The formation of the final stable soliton molecule from background noise requires only 540 RTs [dashed rectangle in Fig. 5(b)], corresponding to a 21 μs intra-cavity travel time.

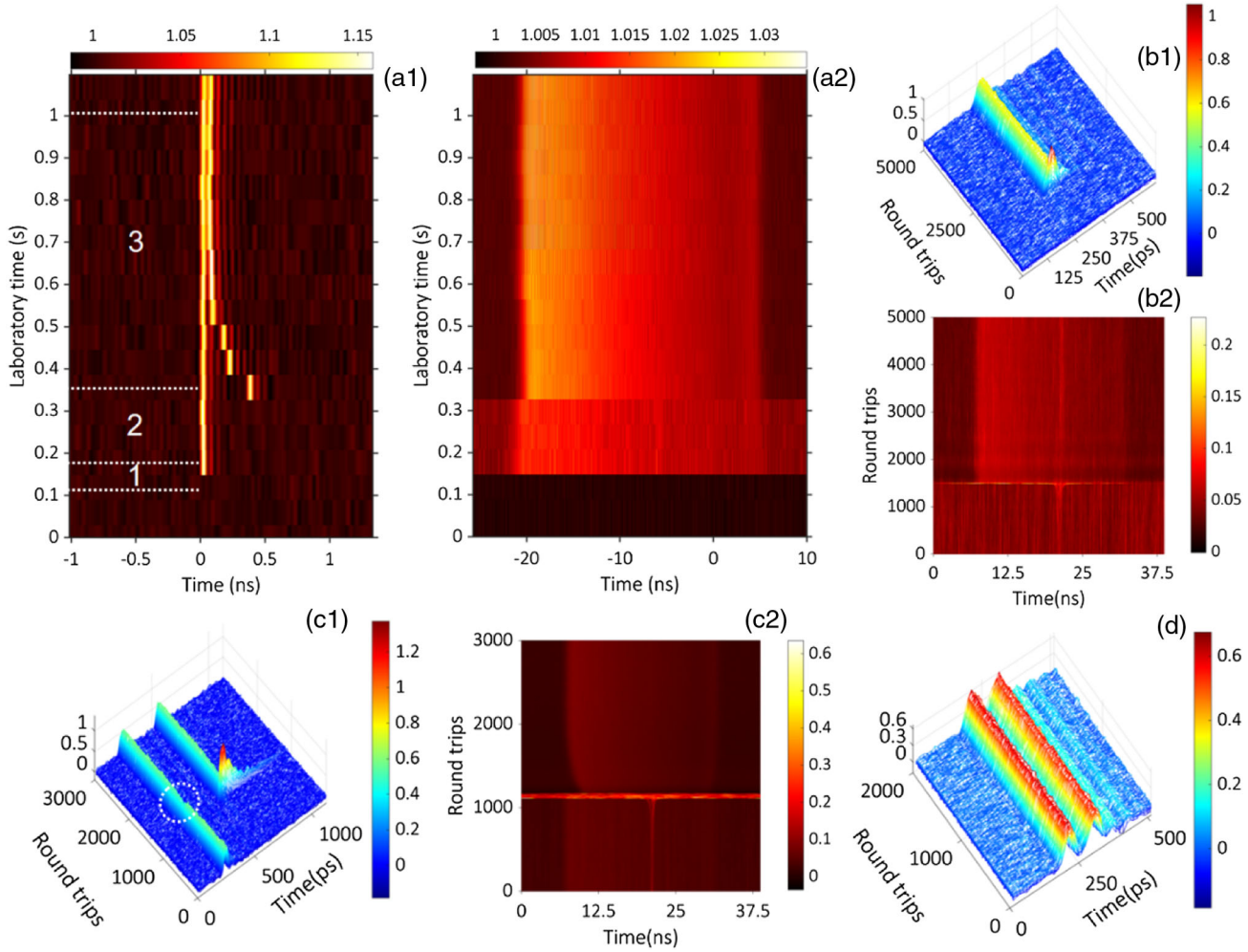

Fig. 6. Long-time soliton molecule formation from background noise. (a1) The temporal intensity evolution of the soliton molecule buildup process measured by a photodetector. (a2) The corresponding spectral evolution measured via DFT. (b1) The temporal intensity evolutions of single soliton formation from noise. (b2) The corresponding real-time spectral evolution measured via DFT. (c1) The temporal intensity evolution corresponds to the process where the single soliton splits into two. (c2) The corresponding real-time spectral evolution measured via DFT. (d) The temporal intensity evolution suggests soliton separation of 100 ps.

B. Long-Time Soliton Molecule Formation Dynamics

In contrast to the short-time soliton molecule buildup process that takes place within hundreds of RTs (~microseconds), the formation time for long-time soliton dynamics increases by several orders of magnitude on the order of several seconds. It is also interesting to understand the formation dynamics of such long-time soliton molecules buildup. To this end, by carefully turning the PCs, we observed the long-time soliton molecule formation process. In order to capture this long dynamic process for 1s, we measured the experimental data not at the repetition rate, but at the interval of ~60 ms. Therefore, the pulse evolution with 50 ps temporal resolution spans over long durations up to several seconds. In this way, we can observe the whole trend of pulse evolution. The recorded TS-DFT data and the corresponding temporal intensity evolutions are shown in Figs. 6(a2) and 6(a1), respectively. In the long-time buildup process, first, a single soliton formed from noise in the time domain (stage 1), then the single soliton split into two solitons with an initial pulse separation of 325 ps (stage 2), and attraction dominates the interaction between the pulses that last for 650 ms. Finally, a stable soliton molecule formed with a pulse separation of 41 ps (stage 3). The whole time for this soliton molecule buildup process is 900 ms, which is over four orders of magnitude longer than that of short-time soliton molecule buildup (21 μs).

In order to observe more details of this dynamics process, we adopted a variable hold-off trigger method to capture different segments of the formation process with 6.4 ms time window for each segment and captured the real-time data at the repetition rate. Thanks to the great reproducibility of this formation process, the experimental results of multiple captures are well consistent. The measured DFT data and corresponding temporal intensity evolutions shown in Figs. 6(b2) and 6(b1) indicate that a single pulse is formed first, which is distinct from the short-time buildup process. Figures 6(c1) and 6(c2) show that a single soliton split into two solitons. The new right pulse evolves into a second femtosecond (fs) pulse via mode-locking; meanwhile, a significant decrease in intensity of the original pulse (marked with a white dashed circle) indicates the new birth pulse effectively splitting the energy of the original pulse. During the attraction phase, the soliton separation of 100 ps corresponds to the temporal intensity evolution shown in Fig. 6(d). At this stage, the interference fringes can be observed on the DFT spectrum, indicating that the two solitons enter the binding state.

Figure 7(a) shows the TS-DFT spectra of the final stable soliton molecule. The zoom-in plot between 1560–1565 nm corresponds to the transparent rectangle shown in Fig. 7(a), as displayed in Fig. 7(d), a slightly sliding phase is readily observed during pulse evolution, and the sliding direction is opposite the short-time buildup process. The field autocorrelation trace [Fig. 7(b)] calculated by the Fourier transformation of Fig. 7(a) suggests that the pulse interaction is stable with a pulse separation of ~41 ps. The stable pulse separation has also been corroborated in the temporal intensity evolution captured by the photodetector [Fig. 7(c)].

In the Ti:sapphire laser, a repeated shedding of smaller fractions [picosecond (ps) pulses] from the original fs pulse in the time domain with a separation of ~1 ns and such a weak ps pulse will eventually evolve into a second fs pulse via mode-locking [26]. The final stable separation between the two solitons is only hundreds of fs. In contrast, in our ultrafast fiber laser operating under normal dispersion, there is no shedding of the smaller fractional ps pulses during the splitting of a single soliton. Two solitons gradually

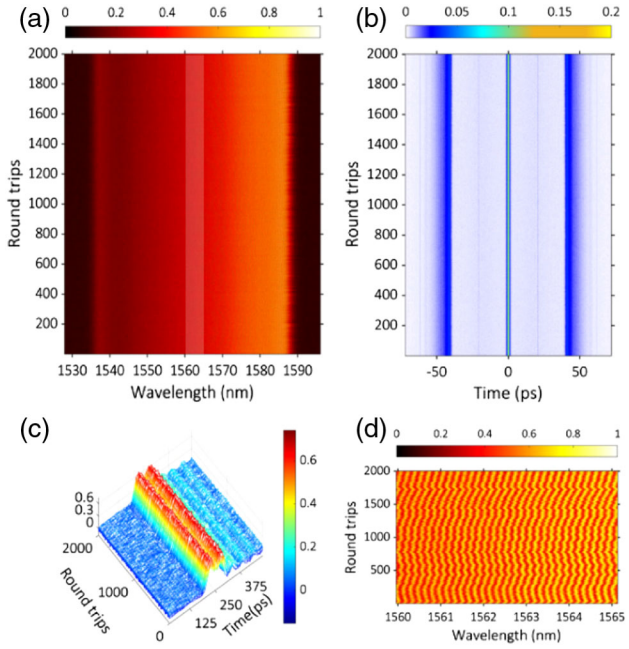

Fig. 7. (a) Real-time spectrum evolution of a stable soliton molecule measured by TS-DFT. (b) The field autocorrelation map calculated via the Fourier transform of each single-shot spectra. (c) The corresponding temporal intensity evolution measured by a photodetector. (d) Zoom-in plot of (a) between 1560 nm and 1565 nm wavelength.

attract each other from 325 ps to 41 ps, undergoing longer attractive time up to 650 ms, and end up as a weak interaction soliton molecule instead of tight binding that only separates hundreds of fs in the Ti:sapphire laser. Our observation suggests that there is an evident difference between the all-fiber mode-locked laser and the Ti:sapphire laser. In addition, similar to the observed soliton molecule, the twin pattern with an extremely long lifetime was reported in the vector rogue wave dynamics in a fiber laser [38]. However, the twin pattern occurs in a unidirectional ring cavity fiber laser without a SA, and the interaction mechanism of solitons is attributed to the interaction between polarization modes in the absence of a SA, which significantly differs from the interaction between solitons influenced by the SA transmission function in this experiment.

C. Soliton Molecule Dissociation Dynamics

In addition to the soliton molecule buildup at short and long time scales, we also observed the soliton molecule dissociation process. In this state, a soliton molecule quickly transits into an unstable single soliton and eventually annihilates. Figure 8(a) shows the DFT spectra exhibiting evident changes of soliton molecule dissociation. The spectra between 1560–1565 nm [marked by the white rectangle in Fig. 8(a)] suggests a significant oscillation phase during evolution [Fig. 8(c)]. Figure 8(b) shows the field autocorrelation traces calculated via the Fourier transforms of each single-shot spectrum. Before the soliton molecule dissociates, there is a relatively obvious change in pulse separation. Figure 8(d) shows the corresponding temporal intensity evolutions measured by the photodetector. The magnified version of the dashed rectangle in Fig. 8(d) illustrates that the two solitons do not merge when the soliton molecule dissociates. The leading soliton transient annihilation, energy transfer, and trailing soliton temporal drift

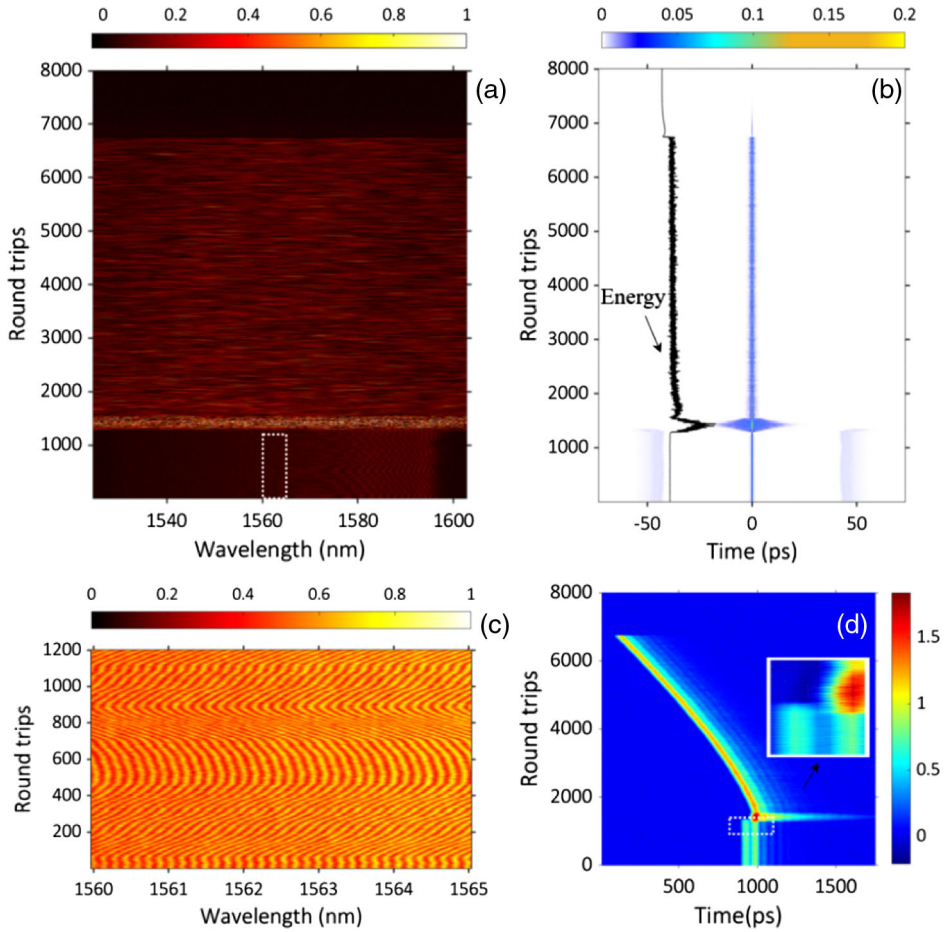

Fig. 8. Soliton molecule dissociation process. (a) The real-time spectral evolution measured via DFT. (b) The field autocorrelation traces calculated via the Fourier transform of each single-shot spectra in (a), the black line shows the energy evolution. (c) Zoom-in plot of the dashed rectangle in (a). (d) The corresponding temporal intensity evolution measured by a photodetector.

agreed well with the simulation [Fig. 3(a)]. From the field autocorrelation traces and temporal intensity evolutions [Figs. 8(b) and 8(d)], during the soliton molecule dissociation, the leading pulse is instantly extinguished, and the energy is transferred to the trailing pulse. Then, a single ps pulse of long soliton tail corresponding to 750 ps is formed, which becomes a weaker pulse with a shorter soliton tail after transmitting 250 RTs. Finally, the weaker single soliton annihilates after transmitting 5200 RTs. Meanwhile, the temporal drift of ~0.9 ns of the single soliton during transmission is caused by the changes in group velocity induced by the evolving central wavelength [39]. The energy evolution by integrating the measured spectra over the complete spectra band [black line in Fig. 8(b)] suggests an energy overshoot when soliton molecules dissociate into a wide ps pulse. Before the single soliton finally annihilates, the energy keeps oscillating, indicating that the single soliton is unstable. At the RT number of 6750, the further decline in energy indeed suggests the extinguishing of the single soliton.

Unlike the soliton molecule that dissociates into a single soliton through repulsive interaction [40] or the soliton molecules that directly annihilate each other [41], in contrast, this work shows a different interaction of a soliton molecule, namely the leading soliton transient annihilation and energy transfer. The extinction of the final single soliton due to the amplitude of soliton below a critical value causes the pulse to experience loss and decay to zero [41,42]. To the best of our knowledge, the exotic soliton molecule dissociation process has not been reported before.

4. CONCLUSION

In conclusion, we reveal the buildup and dissociation dynamics of dissipative soliton molecules in the normal dispersion mode-locked fiber laser. The theoretical prediction is confirmed well by the experimental result of short-time soliton molecule buildup and a new soliton molecule dissociation process. These different dynamical processes are mainly influenced by the polarization-dependent transmission functions of NPR. The gain/loss dynamics also play an important role in soliton molecule buildup and dissociation. In the short-time buildup phase, repulsion dominates the interaction of soliton molecules due to large initial pulse intensity differences and small initial pulse separation. In the long-time buildup phase, there is a splitting of the single soliton, soliton energy transfer, and attraction that dominates the interaction of soliton molecules. For the newly found soliton molecule dissociation process, there exists a soliton transient annihilation and energy transfer instead of two solitons merging, with the annihilation of the final single soliton due to the strength of the soliton below a stable critical value. It is also important to note that these dynamics can obviously differ in different net cavity dispersion and laser systems (such as SA mode-locked fiber laser [43], ultrafast Ti:sapphire lasers [26], and microresonator [44]),

apart from the outside perturbation (the change of the polarization state and the fluctuation of pump power). We believe that our results unveil new perspectives into the soliton molecule transient dynamics of mode-locked lasers and will provide useful insights into laser design and applications.

Funding. Research Grants Council of the Hong Kong Special Administrative Region (CityU T42-103/16-N, E-HKU701/17, HKU 17200219, HKU 17209018, HKU C7047-16G); National Natural Science Foundation of China (N_HKU712/16).

Disclosures. The authors declare no conflicts of interest.

REFERENCES

1. T. Dauxois and M. Peyrard, *Physics of Solitons* (Cambridge University, 2006).
2. N. J. Zabusky and M. D. Kruskal, "Interaction of "solitons" in a collisionless plasma and the recurrence of initial states," Phys. Rev. Lett. **15**, 240–243 (1965).
3. B. Kibler, J. Fatome, C. Finot, G. Millot, F. Dias, G. Genty, N. Akhmediev, and J. M. Dudley, "The Peregrine soliton in nonlinear fibre optics," Nat. Phys. **6**, 790–795 (2010).
4. D. R. Solli, C. Ropers, P. Koonath, and B. Jalali, "Optical rogue waves," Nature **450**, 1054–1057 (2007).
5. J. Denschlag, J. E. Simsarian, D. L. Feder, C. W. Clark, L. A. Collins, J. Cubizolles, L. Deng, E. W. Hagley, K. Helmerson, W. P. Reinhardt, S. L. Rolston, B. I. Schneider, and W. D. Phillips, "Generating solitons by phase engineering of a Bose–Einstein condensate," Science **287**, 97–101 (2000).
6. N. Akhmediev and A. Ankiewicz, eds., "Dissipative solitons in the complex Ginzburg–Landau and Swift–Hohenberg equations," in *Dissipative Solitons* (Springer, 2005).
7. F. Kurtz, C. Ropers, and G. Herink, "Resonant excitation and all-optical switching of femtosecond soliton molecules," Nat. Photonics **14**, 9–13 (2020).
8. A. Klein, G. Masri, H. Duadi, K. Sulimany, O. Lib, H. Steinberg, S. A. Kolpakov, and M. Fridman, "Ultrafast rogue wave patterns in fiber lasers," Optica **5**, 774–778 (2018).
9. Y. Yu, Z. C. Luo, J. Kang, and K. K. Wong, "Mutually ignited soliton explosions in a fiber laser," Opt. Lett. **43**, 4132–4135 (2018).
10. J. Peng and H. Zeng, "Triple-state dissipative soliton laser via ultrafast self-parametric amplification," Phys. Rev. Appl. **11**, 044068 (2019).
11. A. Mahjoubfar, D. V. Churkin, S. Barland, N. Broderick, S. K. Turitsyn, and B. Jalali, "Time stretch and its applications," Nat. Photonics **11**, 341–351 (2017).
12. K. Krupa, K. Nithyanandan, U. Andral, P. Tchofo-Dinda, and P. Grelu, "Real-time observation of internal motion within ultrafast dissipative optical soliton molecules," Phys. Rev. Lett. **118**, 243901 (2017).
13. Z. Q. Wang, K. Nithyanandan, A. Coillet, P. Tchofo-Dinda, and P. Grelu, "Optical soliton molecular complexes in a passively mode-locked fibre laser," Nat. Commun. **10**, 830 (2019).
14. J. Igbonacho, K. Nithyanandan, K. Krupa, P. T. Dinda, P. Grelu, and A. B. Moubissi, "Dynamics of distorted and undistorted soliton molecules in a mode-locked fiber laser," Phys. Rev. A **99**, 063824 (2019).
15. A. Zavyalov, R. Iliew, O. Egorov, and F. Lederer, "Dissipative soliton molecules with independently evolving or flipping phases in mode-locked fiber lasers," Phys. Rev. A **80**, 043829 (2009).
16. X. Liu, X. Yao, and Y. Cui, "Real-time observation of the buildup of soliton molecules," Phys. Rev. Lett. **121**, 023905 (2018).
17. F. Meng, C. Lapre, C. Billet, G. Genty, and J. M. Dudley, "Instabilities in a dissipative soliton-similariton laser using a scalar iterative map," Opt. Lett. **45**, 1232–1235 (2020).
18. M. Stratmann, T. Pagel, and F. Mitschke, "Experimental observation of temporal soliton molecules," Phys. Rev. Lett. **95**, 143902 (2005).
19. M. Pang, W. He, X. Jiang, and P. S. J. Russell, "All-optical bit storage in a fibre laser by optomechanically bound states of solitons," Nat. Photonics **10**, 454–458 (2016).
20. A. I. D'yachenko, V. E. Zakharov, A. N. Pushkarev, V. F. Shvets, and V. V. Yan'kov, "Soliton turbulence in nonintegrable wave systems," Zh. Eksp. Teor. Fiz **96**, 2026–2032 (1989).
21. F. X. Kärtner, J. A. D. Au, and U. Keller, "Mode-locking with slow and fast saturable absorbers—what's the difference?" IEEE J. Sel. Top. Quantum Electron. **4**, 159–168 (1998).
22. D. Y. Tang, L. M. Zhao, B. Zhao, and A. Q. Liu, "Mechanism of multisoliton formation and soliton energy quantization in passively mode-locked fiber lasers," Phys. Rev. A **72**, 043816 (2005).
23. Y. Cui and X. Liu, "Revelation of the birth and extinction dynamics of solitons in SWNT-mode-locked fiber lasers," Photon. Res. **7**, 423–430 (2019).
24. X. Liu and Y. Cui, "Revealing the behavior of soliton buildup in a mode-locked laser," Adv. Photon. **1**, 1–14 (2019).
25. J. Peng and H. Zeng, "Build-up of dissipative optical soliton molecules via diverse soliton interactions," Laser Photon. Rev. **12**, 1800009 (2018).
26. G. Herink, F. Kurtz, B. Jalali, D. R. Solli, and C. Ropers, "Real-time spectral interferometry probes the internal dynamics of femtosecond soliton molecules," Science **356**, 50–54 (2017).
27. V. V. Afanasjev and N. N. Akhmediev, "Soliton interaction in nonequilibrium dynamical systems," Phys. Rev. E **53**, 6471–6475 (1996).
28. B. A. Malomed, "Bound solitons in the nonlinear Schrödinger–Ginzburg–Landau equation," Phys. Rev. A **44**, 6954–6957 (1991).
29. Y. Wang, F. Leo, J. Fatome, M. Erkintalo, S. G. Murdoch, and S. Coen, "Universal mechanism for the binding of temporal cavity solitons," Optica **4**, 855–863 (2017).
30. J. N. Kutz, B. C. Collings, K. Bergman, and W. H. Knox, "Stabilized pulse spacing in soliton lasers due to gain depletion and recovery," IEEE J. Quantum Electron. **34**, 1749–1757 (1998).
31. K. Sulimany, O. Lib, G. Masri, A. Klein, M. Fridman, P. Grelu, O. Gat, and H. Steinberg, "Bidirectional soliton rain dynamics induced by Casimir-like interactions in a graphene mode-locked fiber laser," Phys. Rev. Lett. **121**, 133902 (2018).
32. J. Peng, M. Sorokina, S. Sugavanam, N. Tarasov, D. V. Churkin, S. K. Turitsyn, and H. Zeng, "Real-time observation of dissipative soliton formation in nonlinear polarization rotation mode-locked fibre lasers," Commun. Phys. **1**, 20 (2018).
33. X. Liu and M. Peng, "Revealing the buildup dynamics of harmonic mode-locking states in ultrafast lasers," Laser Photon. Rev. **13**, 1800333 (2019).
34. K. K. Tsia, K. Goda, D. Capewell, and B. Jalali, "Performance of serial time-encoded amplified microscope," Opt. Express **18**, 10016–10028 (2010).
35. R. Xia, Y. Luo, P. P. Shum, W. Ni, Y. Liu, H. Q. Lam, Q. Sun, X. Tang, and L. Zhao, "Experimental observation of shaking soliton molecules in a dispersion-managed fiber laser," Opt. Lett. **45**, 1551–1554 (2020).
36. G. P. Agrawal, *Nonlinear Fiber Optics* (Academic, 2007).
37. K. Goda and B. Jalali, "Dispersive Fourier transformation for fast continuous single-shot measurements," Nat. Photonics **7**, 102–112 (2013).
38. S. A. Kolpakov, H. Kbashi, and S. V. Sergeyev, "Dynamics of vector rogue waves in a fiber laser with a ring cavity," Optica **3**, 870–875 (2016).
39. X. Wang, Y. G. Liu, Z. Wang, Y. Yue, J. He, B. Mao, R. He, and J. Hu, "Transient behaviors of pure soliton pulsations and soliton explosion in an L-band normal-dispersion mode-locked fiber laser," Opt. Express **27**, 17729–17742 (2019).
40. X. Wang, J. He, B. Mao, H. Guo, Z. Wang, Y. Yue, and Y. Liu, "Real-time observation of dissociation dynamics within a pulsating soliton molecule," Opt. Express **27**, 28214–28222 (2019).
41. J. K. Jang, M. Erkintalo, K. Luo, G.-L. Oppo, S. Coen, and S. G. Murdoch, "Controlled merging and annihilation of localised dissipative structures in an ac-driven damped nonlinear Schrödinger system," New J. Phys. **18**, 033034 (2016).
42. J. M. Soto-Crespo, N. Akhmediev, and G. Town, "Continuous-wave versus pulse regime in a passively modelocked laser with a fast saturable absorber," J. Opt. Soc. Am. B **19**, 234–242 (2002).
43. Y. Zhou, W. Lin, H. Cheng, W. Wang, T. Qiao, Q. Qian, S. Xu, and Z. Yang, "Composite filtering effect in a SESAM mode-locked fiber laser with a 3.2-GHz fundamental repetition rate: switchable states from single soliton to pulse bunch," Opt. Express **26**, 10842–10857 (2018).
44. D. C. Cole, E. S. Lamb, P. D. Haye, S. A. Diddams, and S. B. Papp, "Soliton crystals in Kerr resonators," Nat. Photonics **11**, 671–676 (2017).